Journal of Applied Polymer Science

Compatibilization of Natural Rubber/High Density Polyethylene Thermoplastic Vulcanizate with Graphene Oxide through Ultrasonically Assisted Latex Mixing

Ning Yan,[1] Hesheng Xia,[1] Jinkui Wu,[1] Yanhu Zhan,[1] Guoxia Fei,[1] Chen Chen[2]

[1]State Key Laboratory of Polymer Materials Engineering, Polymer Research Institute, Sichuan University, Chengdu 610065, China
[2]Analytical and Testing Centers, Sichuan University, Chengdu 610065, China

Correspondence to: H. Xia (E-mail: xiahs@scu.edu.cn) or C. Chen (E-mail: cdcc@scu.edu.cn)

ABSTRACT: Natural rubber (NR)/high density polyethylene (HDPE) thermoplastic vulcanizate was compatibilized with graphene oxide (GO) by an ultrasonically assisted latex mixing process (ULM). GO was dispersed into NR latex by ultrasonic irradiation and followed by latex coagulation to obtain the NR/GO master-batch, which was further mixed and diluted with HDPE and NR via a dynamic vulcanization process to obtain the NR/HDPE/GO hybrid composites. It was found that the stacked GO platelets were successfully exfoliated by the ULM process and have good compatibilization efficiency for the immiscible NR and HDPE. A smaller discrete NR domain was observed in NR/HDPE blend in the presence of the GO. Moreover, the stacked GO platelets enhance the interfacial adhesion and phase compatibility, which results in an increase in mechanical property of NR/HDPE blends. Compared to the NR/HDPE blend, the tensile strength and tensile modulus at 300% strain for NR/HDPE/ (1.5 phr) GO blend were increased by $\sim$ 27% and $\sim$ 24%, respectively. The exfoliated GO can act as both the effective reinforcing filler and compatibilizer in the immiscible NR/HDPE blend. © 2012 Wiley Periodicals, Inc. J. Appl. Polym. Sci. 000: 000–000, 2012

KEYWORDS: graphene oxide; thermoplastic natural rubber; compatibilization; latex mixing

Received 15 May 2011; accepted 10 April 2012; published online
DOI: 10.1002/app.37861

INTRODUCTION

The combination of different polymers is a fascinating and practical channel to get new materials with novel functions that the individual components do not possess. Thermoplastic natural rubber (TPNR) consisting of natural rubber (NR) and high density polyethylene (HDPE) belongs to such a material with multifunctions. TPNR not only exhibits the conventional properties of elastomeric materials at room and service temperatures but can also flow at elevated temperature and again solidify when the temperature returns, which behaves like thermoplastic HDPE.[1] With the combination of good processing character of HDPE and elastic properties of NR, TPNR can be used in automobile components and other industrial applications.

However, due to mismatch of the polarity, melt viscosity, and molecular weight, the interface adhesion of NR and HDPE is poor, leading to an inferior mechanical property which limits the application. Therefore, it is necessary to improve the compatibilization of two phases. Previous studies used either phenolic resin (i.e., SP-1045 and HRJ-10518) or modified phenolic resins (PhSP-PE and PhHRJ-PE) as compatibilizer or *in situ* reactive compatibilizers to improve interfacial adhesion and to reduce the dispersed domain size in TPNR[2,3]. Liquid natural rubber was also used as the compatibilizer in TPNR.[4,5] It functions both as a cross-linking agent within the NR phase and as an interfacial binder between NR and PE phases to improve the interaction of the binary phase. Both of the strategies above were effective to achieve the compatibilizing of the immiscible polymer blend. However, the compatibilizing efficiency still needs to improve.

In recent years, it was reported that the anisotropic nanofillers which have a large specific surface area and high aspect ratio such as carbon nanotubes and organoclay can also be used as compatibilizers to improve the compatibility of the immiscible polymer blends. For instance, Cheng et al.[6] reported that the incorporation of carboxyl multiwalled carbon nanotubes into PA6/LCP blend resulted in transforming the globular LCP phase into microfibril, indicating a significant improvement in their miscibility and interfacial adhesion between PA6 and LCP. Wu et al.[7] reported a selective localization of carboxyl multiwalled carbon nanotubes in the PLA/PCL and found that the phase

morphology of the ternary CNTs /PLA/PCL composites changed remarkably in contrast to the blank PLA/PCL.

The investigation on the compatibilizer role of the organoclay was well conducted[8–17]. Gelfer et al.[9] showed that the domain size for PS/PMMA blend was dramatically reduced with the addition of organoclay. They ascribed this behavior to the partial compatibilization between the excessive surfactant in organoclays and polymer matrix. Wang et al.[10] suggested that the clay platelets with the intercalated two immiscible polymer chain can act as either a block or graft copolymer to reduce the domain size in PS/PP blend. Ray et al.[12] showed that the exfoliated silicate layers dispersed around the PS phase, inhibits the coalescence of the PS domains, and thus leads to a largely decrease of the dispersed phase size and increase of the mechanical properties.

To understand the compatibilizing effect of inorganic fillers, two possible mechanisms were proposed. Mechanism I (thermodynamic compatibility): with a large specific area and high aspect ratio, anisotropic inorganic nanofillers can absorb the polymer chains on its surface to gain stabilizing energy which make the overall free-energy of mixing (ΔG_m) negative and thermodynamically driven compatibility between the immiscible components.[18] Mechanism II (kinetic compatibility): the selective localization of nanofiller in the polymer interface decreases the interfacial tension and prevents the coalescence of the domains during melt mixing which kinetically improves the compatibility between the binary phases.[7,12] Therefore, the addition of anisotropic nanofillers may bring about the reinforcing and compatibilization effects for an immiscible blend system simultaneously, which is a new approach to achieve high performance of polymer blend nanocomposites.

As a two-dimensional layered carbon nanomaterial, graphene oxide (GO) has gained much attention due to its unique structure and properties in recent years. Normally, it is oxidized from natural flake graphite and consisted of parallel pseudo two-dimensional lamellaes. Exfoliated single GO sheet has been predicted to have strong mechanical strength by Monte Carlo simulations.[19] The GO layers consist of randomly distributed unoxidized aromatic regions and hexahydric aliphatic regions attached with polar groups, such as hydroxyl, epoxide, ether, and carboxylate groups, as a result of oxidation. GO is partially hydrophilic compared to the graphene and can be readily dispersed in water as individual sheets to form stable colloidal suspensions.[20] However, it is still difficult to disperse and exfoliated in the solid polymer matrix. Some methods including the polymerization in the galleries between the carbon layers[21,22] and hydrophobic modification of GO[23,24] were designed for the delamination of carbon sheets in the polymer matrix. Although the intercalated and exfoliated polymer/GO nanocomposites were successfully obtained,[22,23,25–29] however, up to now, few work concerned the compatibilizing effect of GO in polymer blends. Compared to clay, GO, as one of lamellar fillers possesses much higher mechanical properties and has a larger specific surface area, which can maximize the interfacial contact between polymer and fillers, and thus has the potential to be the effective reinforcing filler and the compatibilizer.

In this work, a new attempt was made to disperse and exfoliate the GO layers by ultrasonically assisted latex mixing (ULM) followed by coagulation to prepare the exfoliated GO/NR master-batch. The GO-filled NR/HDPE composites were prepared through further dilution and mixing of the master-batch in NR and HDPE via a dynamic vulcanization process. The feasibility of the proposed ULM process, the morphology and mechanical properties of the obtained NR/HDPE/GO nanocomposites, and the compatibilizing effect of the exfoliated GO in TPNR were investigated.

EXPERIMENTAL

Materials

NR (SCR5) was purchased from Yunnan Natural Rubber Industry Co., Kunming, China. The HDPE (YGH041) used as a blend component was manufactured by Shanghai Petrochemical Company Limited. NR latex (solid content: 60 wt %) was provided by Chengdu Fangzheng Co., (China). Flake Graphite ($\sim$ 75 μm) was obtained from Qingdao Tianhe Graphite Co., (China). Potassium permanganate ($KMnO_4$) was obtained from Chongqing Boyi Chemical Reagent Co., (China). Concentrated sulfuric acid (H_2SO_4) and hydrochloric acid (HCl) were all analytical-grade and obtained from Sichuan Xilong Chemical Co., (China). Hydrogen peroxide (30%) was provided by Tianjin Zhiyuan Chemical Reagent Co., (China). Formic acid was purchased from Tianjin Bodi Chemical Reagent Co., (China). Other reagents including vulcanization agent sulfur (S), zinc oxide (ZnO), accelerator N-cyclohexyl-2-benzothiazole-sulfenamide (CBS), 2-mercaptobenzothiazole (MBT) and 4-Isopropylamino-diphenylamine (4010NA), and stearic acid (SA) are all commercially available.

Preparation of GO

GO was prepared using Hummer's method.[30] Briefly, $KMnO_4$ (42 g) was added slowly to a flask that contained concentrated H_2SO_4 (300 mL) and flake natural graphite powder (12 g) to make sure that the reaction temperature was controlled below 20°C by immersing the flask in ice-bath. And then, the reaction mixture was stirred for 2 h at 35°C. After that distilled water (552 mL) was slowly fed into the reactor, which made the mixture boil, and the mixture was allowed to stir for another 15 min. To stop the oxidation reaction, 30% H_2O_2 (20 mL), which reduced the excess $KMnO_4$ was fed sequentially into the reactor until there is no bubble. The resultant GO suspension was centrifuged at 12,000 rpm for 5 min. The obtained solid mixture was washed with diluted HCl solution (3 wt %) and distilled water by centrifugation and redispersion for three times. The obtained colloid was dialyzed in the deionized water for a week and dried in a vacuum oven at 50°C for 72 h.

Preparation of NR/GO Master-Batch via a ULM Process

2.5 mg/mL GO aqueous solution was prepared by bath sonication (KQ-250DE, 40 KHz, Kunshan Ultrasonic Instrument Co., China) at 40°C for 1 h.[31] And then, 8.3 g NR latex was dispersed into the GO solution by sonication. After 1 h ultrasonic irradiation, the mixture was coagulated by adding formic acid drop by drop while stirring. The solid was cut and washed to be neutral with water and then was vacuum dried in an oven at 65°C for 24 h to obtain the well dispersed GO/NR master-

Table I. Formulation of the NR/HDPE/GO Composites

Components	REG0	REG0.5	REG1	REG1.5	D-REG1.5
HDPE	40	40	40	40	40
NR	50	50	50	50	50
NR/GO master-batch	L-R	L-RG0.5	L-RG1	L-RG1.5	D-RG1.5
	10	10.5	11	11.5	11.5
Zinc oxide	3	3	3	3	3
Stearic acid	1.2	1.2	1.2	1.2	1.2
Sulfur	1.8	1.8	1.8	1.8	1.8
Antioxidant (4010NA)	1.8	1.8	1.8	1.8	1.8
Accelerator (CBS)	0.9	0.9	0.9	0.9	0.9
Accelerator (MBT)	0.12	0.12	0.12	0.12	0.12

batch, designated as L-RG0.5, L-RG1, and L-RG1.5 corresponding to the GO content of 0.5, 1, and 1.5 phr (phr means parts per hundred parts of thermoplastic rubber) in NR/HDPE composite, respectively. A contrast NR/GO master-batch without ULM treatment designated as D-RG1.5 was also prepared. The self-made blank nature rubber without GO obtained from the rubber latex was designated as L-R.

Preparation of NR/HDPE/GO Composites

NR and HDPE blends were prepared at a fixed blend ratio of NR/HDPE (60/40). Blending was carried out via a melt mixing process using an internal mixer (Haake Rheomix 600 mixer, Germany). The thermoplastic component, HDPE, was first dried in a hot air oven at 50°C for at least 10 h and later introduced into the mixing chamber. Mixing was performed for 2 min at a rotor speed of 60 rpm at 165°C. Then the master-batch prepared by the above ULM process and NR were added into the mixing chamber and mixed for another 2 min. The other ingredients (as shown in Table I) were sequentially added into the mixing chamber and mixed for 4 min. The resultant was then transferred to a twin-roll mill and compounded for additional 5 min at 150°C. Then, the NR/HDPE/GO lump was thermally compressed for 8 min at 150°C under a pressure of 10 MPa with an electrically heated hydraulic press machine and then was cooled for 3 min at room temperature under a pressure of 10 MPa to form the NR/HDPE/GO sheet of 2 mm thickness. The NR/HDPE/GO composites with various contents of GO were named as REG0, REG0.5, REG1, and REG1.5, respectively. A contrast sample 60NR/40HDPE/1.5GO composite was also prepared in the same condition by direct use of D-RG1.5 master-batch without a ULM process. The obtained sample was designated as D-REG1.5.

Characterization

Atomic Force Microscope. Atomic force microscope (AFM) observation was performed in a tapping mode on a NanoScope MultiMode III AFM instrument. The suspensions of a concentration of 0.02 mg/mL GO were prepared by ultrasound for 1 h. Water was used as the dispersion medium. The sample was prepared by depositing the diluted solution on a silicon wafer.

X-ray Photoelectron Spectroscopy. X-ray photoelectron spectroscopy (XPS) measurements were carried out in an XSAM800 (Kratos, Britain) with a pressure 2×10^{-7} Pa in the analysis chamber. The unmonochromated using monochromatic Mg Kα X-ray source radiation ($hv = 1253.6$ eV), operated at 12 KV and 15 mA, was used to measure both photoemission core-level spectra. The electron analyzer was operated in the fixed analyzer transmission (FAT) mode. All spectra were calibrated to binding energy for Cu2P3/2(932.67 eV), Ag3d5/2(368.30 eV), and Au4f7/2(84.00 eV) levels. Charge effects were compensated assuming carbon C1s peak at 284.8 eV position.

X-ray Diffraction. The samples including graphite, GO, GO/NR master-batch, and NR/HDPE/GO composites were mounted individually into a Philip-X'Pert X-ray diffractometer fitted with a goniometer detection device (anode 40 kV, filament current 35 mA). Nickel-filtered CuKα radiation of wavelength 0.1542 nm was directed at the samples in their through direction. The goniometer scanned diffracted X-rays in the 2θ range 5–45° at a scan speed of 0.15°/s.

Scanning Electron Microscope. The blend morphologies were examined by scanning electron microscope (SEM) using an inspect F model FEI apparatus at an accelerating voltage of 10 KV. The samples were fractured in liquid nitrogen. The fractured surfaces were etched by chloroform at 60°C for 1 h to remove the NR phase. And then, the samples were dried in a vacuum oven at 40°C for 3 h and then sputter coated with gold.

Transmission Electron Microscope. Transmission electron microscope (TEM) observation was performed by using a FEI Fecnai G^2 F_{20} S-Twin TEM, operating at an accelerating voltage of 200 kV. For NR/GO latex sample, the latex after dilution for 15 times was directly dropped on a copper grid for observation. For the NR/HDPE and NR/HDPE/GO composites, the samples were cryomicrotomed at −85°C using Leica EM UC6 to get the ultrathin cryosections of 70–80 nm thickness, respectively. To localize the exfoliated GO clearly, the sections of NR/HDPE/GO were stained by osmium tetraoxide (OsO_4) for 20 min.

Differential Scanning Calorimeter. A NETZSH 204 differential scanning calorimeter (DSC) instrument was used to investigate the crystallization of NR/HDPE and its NR/HDPE/GO composites in nitrogen atmosphere. The samples 5–10 mg were first heated from 30 to 180°C at a heating rate of 10°C min^{-1} and then kept at 180°C for 5 min to remove the thermal history.

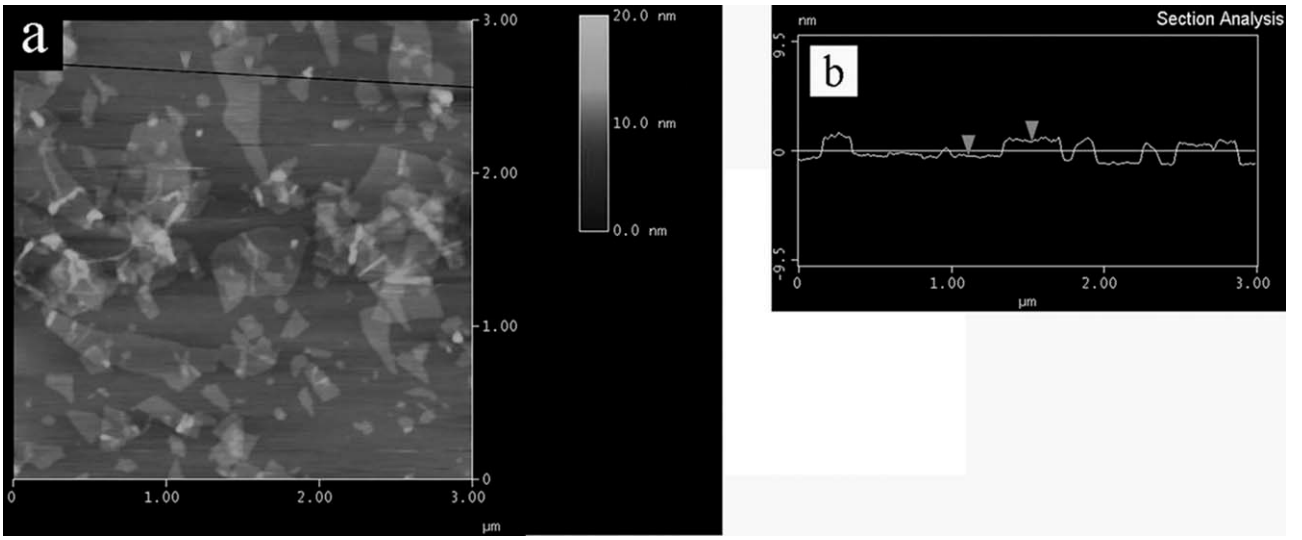

Figure 1. The AFM images (a) graphene oxide and (b) height profiles.

And then, the melt was cooled down to 30°C at a rate of 10°C min^{-1}. The endothermic and the exothermic curves were recorded respectively.

Tensile Properties. The measurement of tensile properties were conducted on a universal testing machine (Instron 5567, MA) at room temperature. For tensile tests, the dumbbell-shaped specimens were stretched until break at a crosshead rate of 500 mm/min according to a China Standard GB/T 528-1998. The stress-strain curves were recorded. The tensile strength, elongation, and stress at the 100, 200, and 300% strain were the average values of five specimens.

RESULTS AND DISCUSSION

Preparation and Characterization of GO

The GO was prepared using Hummer's method.[30] Figure 1 shows the tapping-mode AFM image of the diluted GO suspension with a concentration of 0.02 mg/mL deposited on the silicon wafer. The irregular GO sheets and the corresponding height profiles are shown in Figure 1(a). The uniform thickness of GO is about ~ 1.0 nm as shown in Figure1(b). The results show that the exfoliation of graphite oxide into individual single-layered GO sheets was achieved as expected. Detailed structural and compositional analyses of the GO were undertaken by XPS, which provides quantitative information about the type and extent of surface functionalization. Figure 2 shows survey XPS spectra of the samples GO. The GO layers are composed of randomly distributed unoxidized aromatic regions and hexahydric aliphatic regions attached with oxygen containing groups, such as hydroxyl, epoxy, and carboxyl. The schematic drawing of the structure of GO is represented in Figure 3. The presence of these functional groups makes GO strongly hydrophilic, which allows the layered GO to be readily intercalated by water to push apart and eventually delaminated into a single carbon layer. The ratio of the atom number of C and O (C/O) in the surface for the samples was determined from the ratio of

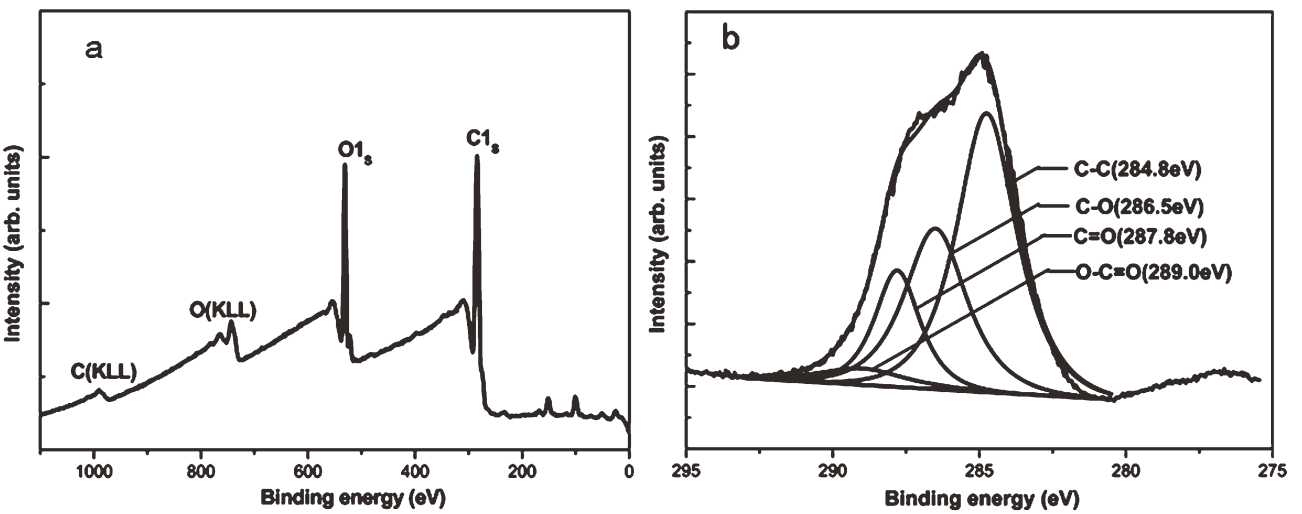

Figure 2. (a) XPS spectra of graphene oxide and (b) C1s peak of graphene oxide.

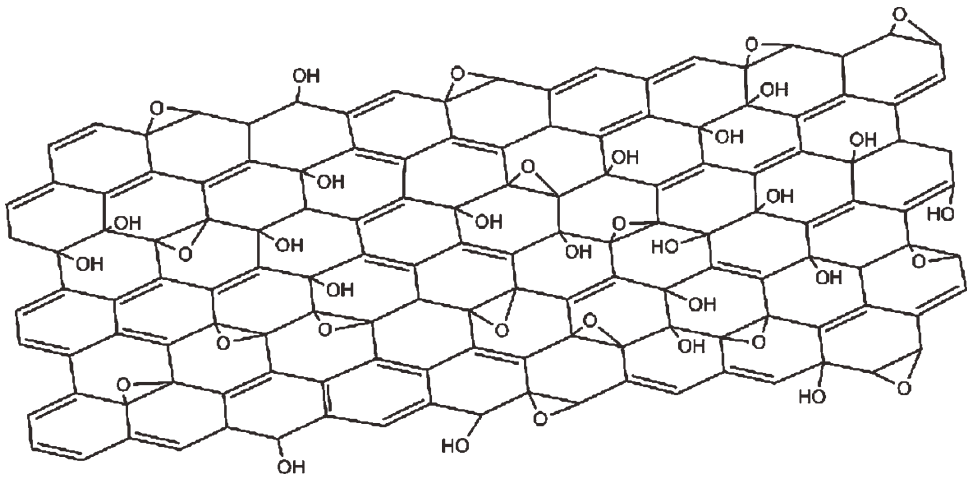

Figure 3. A proposed schematic of the structure of graphene oxide.

peak areas corrected with the empirical sensitivity factors. The C/O ratio for GO is ~ 0.31. This XPS C1s peaks were fitted by a multipeak Lorentzian fitting program (Xpspeak). The fitted curves were shown in Figure 2(b). The relative carbon atom percentages in different functional groups of C—C (284.8 ev), C—O (286.5 ev), C=O (287.8 ev), and O—C=O (289.0 ev) are calculated as 50.3, 29.8, 15.8, and 4.1, respectively. The XPS results coincide with the structure of the GO.

Dispersion and Exfoliation of GO in Rubber Latex

The X-ray diffraction (XRD) pattern of pristine graphite [Figure 4(a)] shows a very intense, sharp peak at $2\theta \sim 26.5°$. This peak corresponds to the diffraction of the (002) graphite plane with an interlayer spacing of d ~ 3.35 Å. Figure 4(b) shows that the peak at d ~ 3.35 Å was not observed in the curve of GO, instead, a new large and broader peak appears around 2θ, ~ 10.6°, corresponding to the (002) plane of GO. This shows that the d-spacing expanded from ~ 3.35 to ~ 8.9 Å by the oxidation, because various functional groups such as hydroxyl and carboxyl groups were introduced on the surfaces of each GO layer. The XRD curve of the L-RG1.5 master-batch was shown in Figure 4(d). The characteristic XRD diffraction peak of pure GO sheets at 2θ, ~ 10.6° disappears, and the broad amorphous peak associated to NR is found at around 2θ, ~ 18.1°. The XRD pattern of the contrast sample D-RG1.5 which is prepared by direct mixing of the GO powder and NR was shown in Figure 4(c). The presence of peak at 2θ, ~ 10.1° suggests that GO layers are not exfoliated without the ULM treatment. In addition, the latex sample L-RG1.5 before coagulation was observed by TEM. The dispersion state of GO in the latex was shown in Figure 5. It can be seen that the NR latex particles are wrapped by the crumpled thin GO sheets. These results suggest that GO sheets are well exfoliated and uniformly dispersed in NR matrix by the ULM process. TEM results are in good agreement with the XRD analysis.

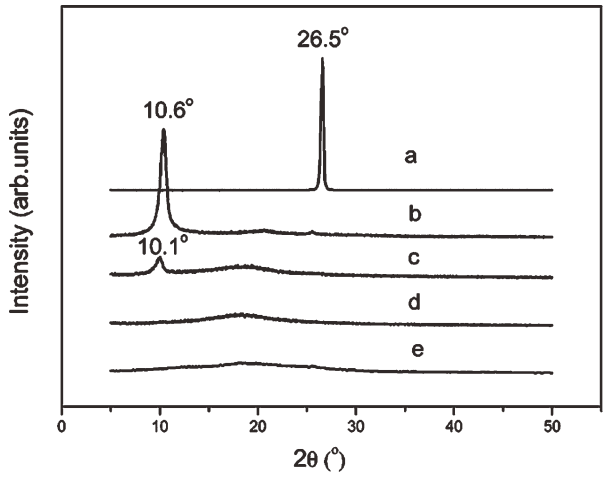

Figure 4. XRD patterns of (a) graphite, (b) GO, (c) RG1.5, (d) L-RG1.5, and (e) NR.

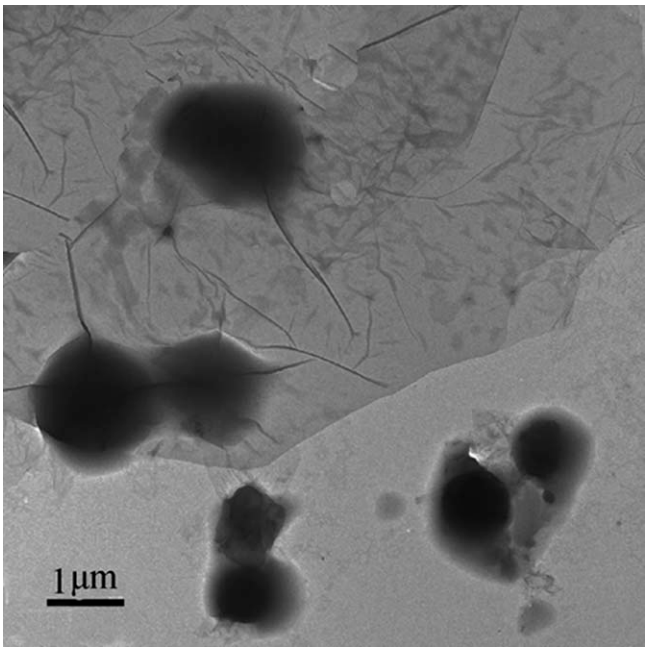

Figure 5. TEM image of the latex sample L-RG1.5 before coagulation.

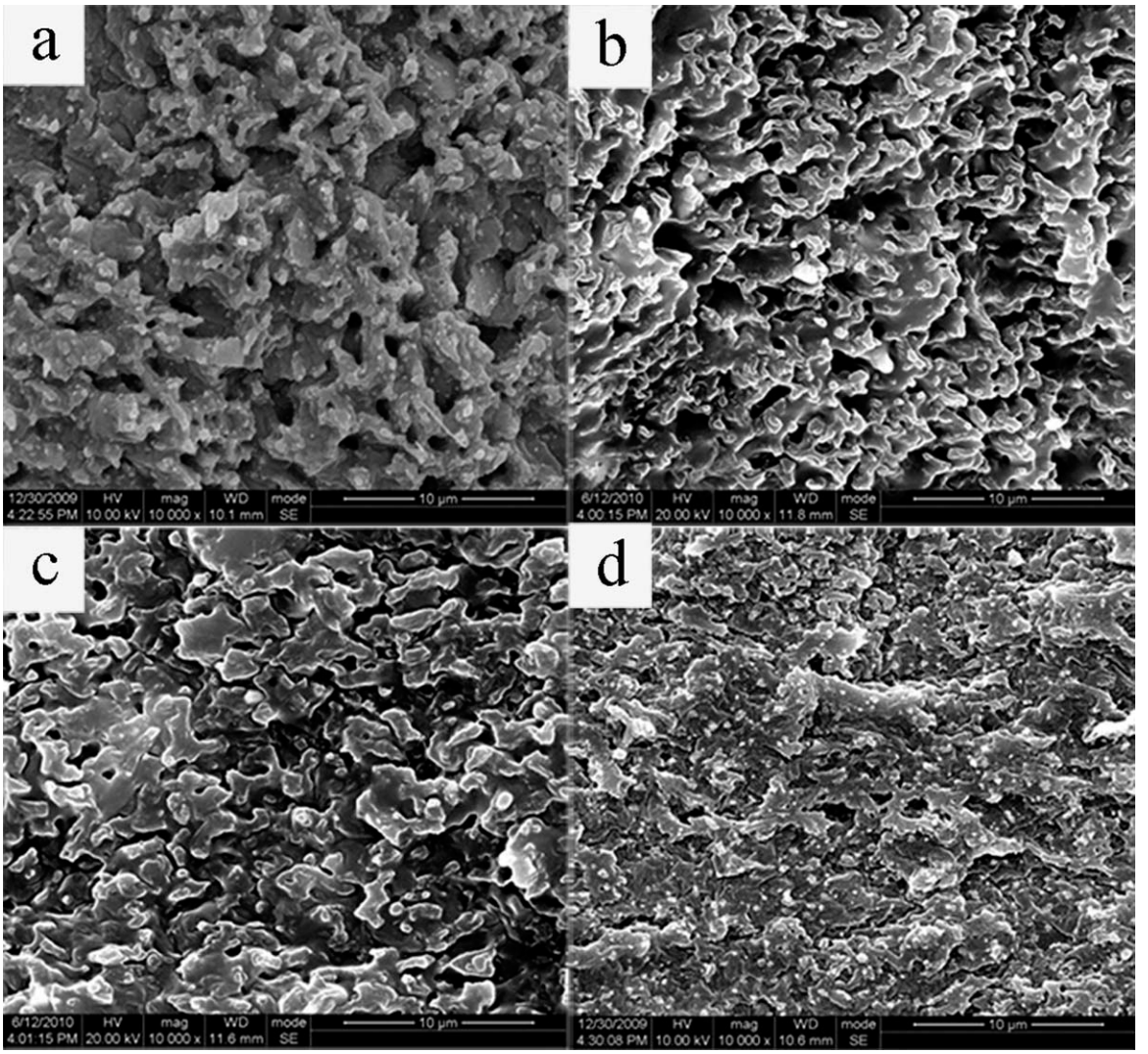

Figure 6. SEM images of the NR/HDPE/GO composites (a) REG0, (b) REG0.5, (c) REG1, and (d) REG1.5.

GO-Induced Compatibilization of NR and HDPE

Figure 6 shows SEM images of the cryofracture surface for NR/HDPE/GO composites with various GO loadings, respectively. Before the SEM observation, the composite's surface was etched by chloroform at 60°C for 1 h to enhance the phase contrast. Clearly, all samples show typical two phase morphology, where the cavities are the etched NR phase indicating the degree of immiscibility of the components. It shows that with the increase of GO content, the average size of NR domains reduces. This suggests an improved interfacial adhesion and phase miscibility. However, some NR phases cannot be etched completely due the crosslinked structure formed during dynamic vulcanization. The morphology of NR phases is not so clear in the SEM images.

To get a deep insight in the phase morphology and GO interfacial activities, TEM was carried out for the selected samples REG0, REG1.5, and D-REG1.5. To enhance the contrast between the phases and to localize the exfoliated GO clearly, REG1.5 was stained by osmium tetraoxide (OsO_4) for 20 min during which the chemical reaction occurs between OsO_4 and the double bonds of the NR. The typical two-phase structure can be seen in Figure 7, in which the dark gray and white areas correspond to NR and HDPE phases, respectively. The incorporation of the GO decreases the size of NR domains and results in finer dispersion of NR in HDPE matrix when comparing Figure 7(a) and (b). The phase compatibility and interfacial adhesion were enhanced, which suggests the good compatibilizing effect of GO in NR/HDPE blend.

At higher magnification, GO sheets are finely dispersed in the matrix as shown in Figure 7(b1). It indicates that delamination of the GO sheets was realized by the ULM method which is consistent with the result of Figure 4(d). In addition, it can be observed that GO are mainly dispersed in the NR phase [Figure 7(b1)] and on the phase interface [Figure 7(b2)]. The selective localization of the fillers such as clay[32,33] and CNTs[6,7,34,35] was also observed in polymer blends in which the two phases show differences in their polarity and affinity to the fillers. In this case, GO platelets premixed in NR latex were wrapped by the NR and thus mainly located in NR matrix with better affinity.

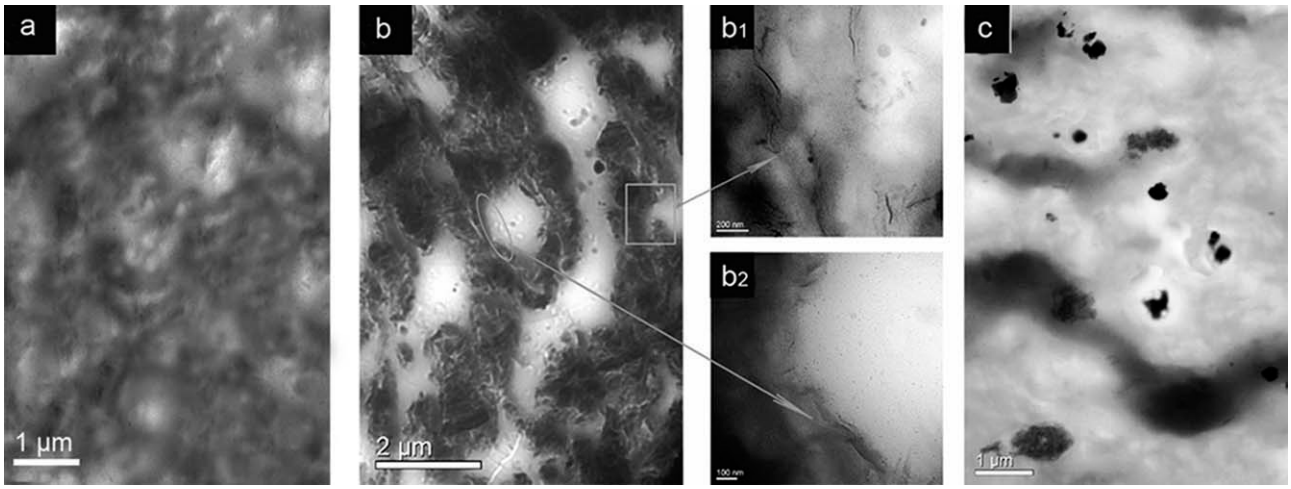

Figure 7. TEM images of NR/HDPE/GO composites (a) REG0, (b) REG1.5 and (c) D-REG1.5. The local regions in picture (b) were magnified as shown in pictures (b_1) and (b_2).

In addition, the GO platelets are further impelled by the mixing flow to disperse and orientate along the interface. The exfoliated GO platelets with a high aspect ratio dispersed at the interface of the binary phase act as barriers, inhibiting the coalescence of the NR domain during the melt mixing. The large aspect ratio and localization at the interface of the blend should be the dominant factors for the nanofiller to have compatibilizing effect. To illustrate the advantage of the ULM process, the contrast sample (D-REG1.5) prepared without the ULM method was also observed by TEM. As shown in Figure 7(c), the aggregated GO particles with an average size of ~ 500 nm can be observed, suggesting that GO powders cannot be dispersed in the rubber matrix in an exfoliation state by direct mixing.

GO-Induced Mechanical Property Improvement of NR/HDPE/GO Composites

Tensile properties for the NR/HDPE/GO composites with different contents of GO are listed in Table II. Figure 8 shows the typical stress-strain curves of the above composites. It can be seen that small addition of GO through the ULM process remarkably enhances the tensile strength of the NR/HDPE composites. Compared to NR/HDPE blend, the tensile strength of NR/HDPE/GO increases from 9.5 to 12.0 MPa with the addition of 1.5 phr GO. Also, the tensile modulus at 100, 200, and 300% strain of the NR/HDPE/GO composites gradually increase with increasing the GO content. This should be attributed to the good dispersion of lamellar GO platelets and the improved compatibilization induced by GO. The interface localization of GO layer improves the phase adhesion, resulting in good load transfer at the interfacial region. A slight decrease in the elongation at break occurs at a higher GO content. Compared to the other compatiblizer, GO has a better compatibilizing effect on NR/HDPE blend and the required amount of GO for reinforcing effect is lower. Nakason et al.[3] prepared NR (60)/HDPE (40) blend by using the modified phenolic resin (PhHRJ-PE) as a compatibilizer, the result showed that the tensile strength increased from 7.5 to 9.5 MPa with the incorporation of ~ 5 wt % PhHRJ-PE. Ahmad et al.[36] reported a reinforcing effect of the hybridized clay and poly (p-phenylene-2,6-benzobisoksazole) PBO fiber on the NR/HDPE blend. The optimum tensile strength ~ 10.5 MPa was obtained with the addition of ~ 12.5 wt % PBO and ~ 7.5 wt % clay.

For the contrast sample D-REG1.5 prepared by direct mixing without using the ULM process, the tensile strength and elongation at break of the resulting composites were much lower than those of the composites prepared using the ULM process (REG1.5). The reason should be that GO powders cannot be effectively dispersed in D-REG1.5 as shown in Figure 6(b) and tend to agglomerate to form the stress concentration points. On the other hand, those GO powders in D-REG1.5 composite were not mainly distributed on the interface, leading to weak

Table II. Tensile Properties of NR/HDPE/GO Composites

Samples	Tensile strength (MPa)	Elongation at break (%)	Stretching stress (MPa)		
			100%	200%	300%
REG0	9.5 ± 0.4	458 ± 16	5.5 ± 0.1	6.5 ± 0.1	7.6 ± 0.1
REG0.5	10.2 ± 0.4	516 ± 7	5.7 ± 0.2	6.8 ± 0.3	7.9 ± 0.4
REG1.0	11.7 ± 0.5	495 ± 5	5.9 ± 0.2	7.0 ± 0.2	8.2 ± 0.3
REG1.5	12.0 ± 0.3	451 ± 41	6.5 ± 0.1	7.9 ± 0.2	9.4 ± 0.4
D-REG1.5	9.5 ± 0.1	382 ± 10	5.3 ± 0.2	6.7 ± 0.2	8.3 ± 0.1

Applied Polymer SCIENCE

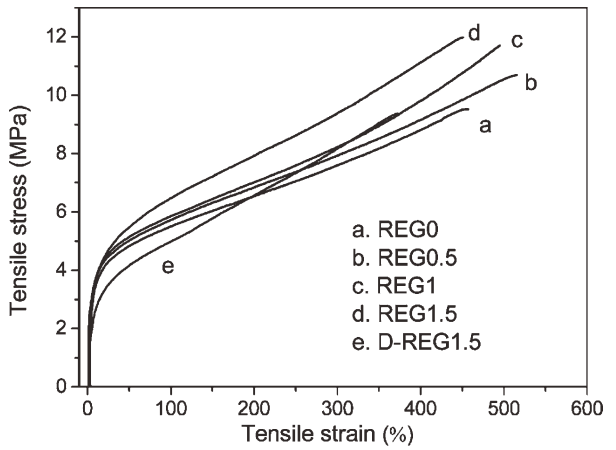

Figure 8. Tensile curves of NR/HDPE/GO composites with different contents of GO.

interfacial adhesion between the NR and HDPE. The results suggest that ULM process is an effective strategy to enhance the dispersion of GO, and further brings about both reinforcing and compatibilizing efficiency of GO in the TPNR blend.

HDPE is a crystalline polymer and its mechanical properties should relate to the crystallinity. To rule out the effect of crystallinity change on the physical properties, DSC and XRD were used to characterize the crystallinity difference between REG0 and REG1.5. Figure 9 represents the DSC curves of the pure HDPE, REG0, and REG1.5. The crystallinity (X_c) of HDPE and its composites were calculated as follows:[37]

$$X_C(\text{HDPE}) = \Delta H(\text{HDPE})/\Delta H_0(\text{HDPE}) \quad (1)$$

$$X_c(\text{REG}) = \Delta H(\text{REG})/\Delta H_0(\text{HDPE}) \quad (2)$$

$$X_C^*(\text{HDPE}) = X_C(\text{REG})/W(\text{HDPE}) \quad (3)$$

Where ΔH (HDPE) and ΔH (REG) represent the apparent enthalpy of fusion per gram for the HDPE and the composites, respectively. ΔH_0 (HDPE) is the heat of fusion per gram for 100% crystalline HDPE, taken as 70 cal/g.[38] As shown in eq. (3), the weight fraction W (HDPE) should be considered in the calculation of the crystallinity of HDPE in the blends (X_C^*(HDPE)). Table III lists the data calculated according to the eqs. (1)–(3). The results show that the melting point of REG1.5 composite is only 1.5°C higher than that of REG0 and the crystallinity of REG1.5 is slightly lower than that of REG0. In addition, with the addition of NR and GO into HDPE, the crystallization temperature decreases when the blends were cooled down. The reason may be that the presence of NR and laminar GO impedes the rearrangement of molecular chain of HDPE melt and suppresses the crystallization of HDPE to some degree during the cooling process.

Table III. DSC Data of Pure HDPE, REG0, and REG1.5 Composites

	$T_{m\ HDPE}$ (°C)	$T_{C\ HDPE}$ (°C)	Crystallinity (%)
HDPE	129.7	118.4	61.7
REG0	131.7	113.3	12.2
REG1.5	133.2	111.8	10.8

Figure 10 shows the XRD patterns of the REG0, REG1.5, and D-REG1.5. The strong peaks at 21.5 and 23.8° correspond to the (110) and (200) lattice planes of HDPE crystal in the composites. The crystallinity is estimated according to the eq. (4):[39]

$$X_C = \frac{A_c}{A_c + A_a} \times 100\% \quad (4)$$

where X_c is the crystallinity, A_c and A_a are the areas of the crystalline region and amorphous region, respectively. The XRD curves were fitted by software JADE5 and the crystallinity of REG0 and REG1.5 were estimated as 23.3 and 22.6%, respectively. There is almost no change in the crystallization of two samples. The discrepancy of the calculated crystallinity between DSC and XRD is mainly attributed to the different test methods. In addition, Figure 10 shows that the characteristic diffraction peaks of GO sheets at 2θ, $\sim 10.6°$ in both REG1.5 and D-REG1.5 disappear. This may be attributed to the low concentration of the GO. The calculated crystallinity of the sample D-

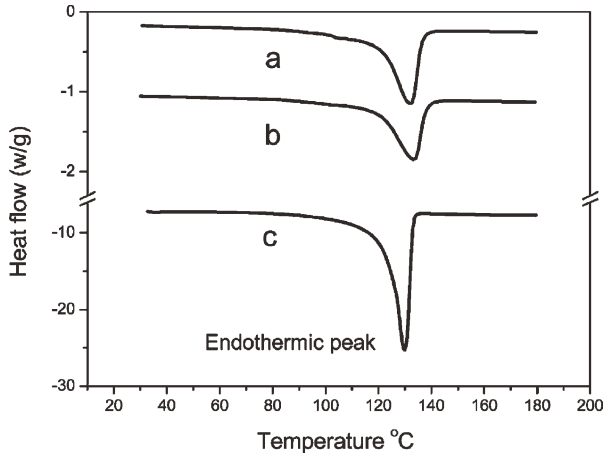

Figure 9. DSC curves of the (a) REG0, (b) REG1.5 and pure HDPE, and (c) composites.

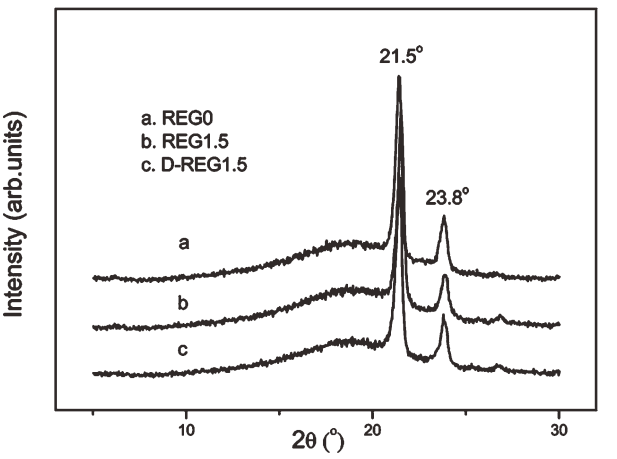

Figure 10. XRD patterns of the (a) REG 0, (b) REG 1.5, and (c) D-REG 1.5 composites.

REG1.5 was ~ 23.9%. So, the discrepancy of HDPE crystallinity caused by the incorporation of GO can be neglected. The significant improvement of the physical properties with the addition of GO by a ULM process should be ascribed to the homogeneous dispersion of GO platelets and the strong interfacial interactions as well as the resulted high stress transfer efficiency among the components.

CONCLUSION

The GO-filled NR/HDPE thermalplastic vulcanizates were successfully prepared by the ULM process and further dynamic vulcanization. The compatibilizing effect of GO on morphology and mechanical property of the blend was investigated. The characteristic XRD diffraction peak of pure GO sheets in NR/GO master-batch disappears, which suggests that the ULM process is an effective strategy to exfoliate GO platelets. The addition of exfoliated GO to the NR/HDPE blend reduces the NR domain size and improves the miscibility and interfacial adhesion between the binary phases. It was found that the GO is mainly dispersed in NR phase and the interface, which acts as an obstacle to inhibit the coalescence of the NR phase. With the addition of 1.5 phr exfoliated GO, the tensile strength of the NR/HDPE composite increases from 9.5 to 12.0 MPa. For the sample prepared by direct mixing without using the ULM process, the tensile strength and elongation at break were lower than those of the composites prepared using the ULM process. The change of HDPE crystallinity due to the incorporation of GO is small and was not the main reason for the improvement in the mechanical properties. The exfoliated GO can act as both the effective reinforcing filler and the compatibilizer in the immiscible NR/HDPE blend. This method proves to be promising and viable to produce the high performance, ultralight thermoplastic vulcanizate.

ACKNOWLEDGMENTS

This project is supported by the National Basic Research Program of China (973 Program 2007CB714701) and International cooperation project of Sichuan province (2010HN0053).

REFERENCES

1. Coran, A. Y. In Handbook of Elastomers-New Developments and Technology; Marcel Dekker: New York, **1998.**
2. Pechurai, W.; Nakason, C.; Sahakaro, K. *Polym. Test.* **2008,** *27*, 621.
3. Nakason, C.; Nuansomsri K.; Kaesaman, A. *Polym. Test.* **2006,** *27*, 782.
4. Jamil, M. S.; Ahmad I.; Abdullah, I. J. *Polym. Res.* **2006,** *13*, 315.
5. Ahmad, S.; Abdullah, I.; Kohjiya, S.; Yoon, J. R. *J. Appl. Polym. Sci.* **1994,** *51*, 1357.
6. Cheng, H.; Sahool, N. G.; Khin, T. H.; Li, L. J. *Nanosci. Nanotechnol.* **2010,** *10*, 5242.
7. Wu, D. F.; Zhang, Y. S.; Zhang, M.; Yu, W. *Biomacromolecules* **2009,** *10*, 417.
8. Voulgaris, D.; Petridis, D. *Polymer* **2002,** *43*, 2213.
9. Gelfer, M.; Song, Y. H.; Liu, L.; Hsiao, B. J. *Polym. Sci. Polym. Phys.* **2003,** *41*, 44.
10. Wang, Y.; Zhang, Q.; Fu, Q. *Macromol. Rapid Commun.* **2003,** *24*, 231.
11. Mehrabzadeh, M.; Kamal, M. R. Can. J. *Chem. Eng.* **2002,** *80*, 1083.
12. Ray, S. S.; Pouliota, S.; Bousminaa, M.; Utrackib, L. A. *Polymer* **2004,** *45*, 8403.
13. Ray, S. S.; Bousmina, M. *Macromol. Rapid Commun.* **2005,** *26*, 450.
14. Ray, S. S.; Bousmina, M. *Macromol. Rapid Commun.* **2005,** *26*, 1639.
15. Khatua, B. B.; Lee, D. J.; Kim, H. Y.; Kim, J. K. *Macromolecules* **2004,** *37*, 2454.
16. Elias, L.; Fenouillot, F. J.; Majeste, C.; Alcouffe, P. *Polymer* **2008,** *49*, 4378.
17. Fenouillot, F.; Cassagnau, P.; Majeste, J. C. *Polymer* **2009,** *50*, 1333.
18. Lipatov, Y. S. Polymer Reinforcement; ChemTec Publishing: Toronto, Canada **1995.**
19. Paci, J. T.; Belytschko, T.; Schatz, G. C. *J. Phys. Chem. C.* **2007,** *49*, 18099.
20. Stankovich, S. D.; Dikin, A.; Piner, R. D.; Jia, Y. *Carbon* **2007,** *7*, 1558.
21. Matsuo, Y.; Tahara, K.; Sugie, Y. *Carbon* **1996,** *34*, 672.
22. Matsuo, Y.; Tahara, K.; Sugie, Y. *Carbon* **1997,** *35*, 113.
23. Matsuo, Y.; Watanabe, K.; Fukutsuka, T.; Sugie, Y. *Carbon* **2003,** *41*, 1545.
24. Liu, P.; Gong, K.; Xiao, P. *Carbon* **1999,** *37*, 2073.
25. Xu, J.; Hu, Y.; Song, L.; Wang, Q.; Fan, W.; Chen, Z. *Carbon* **2002,** *40*, 445.
26. Kovtyukhova, N.; Ollivier, I. P. J.; Martin, B. R. *Chem. Mater.* **1999,** *11*, 771.
27. Kyotani, T.; Moriyama, H.; Tomita, A. *Carbon* **1997,** *35*, 1185.
28. Jang, J. Y.; Kim, M. S.; Jeong, H. M. *Comp. Sci. Tech.* **2009,** *69*, 186.
29. Wang, J.; Han, Z. *Polym. Adv. Technol.* **2006,** *17*, 335.
30. Hummers, W. S.; Offeman, R. E. *J. Am. Chem. Soc.* **1958,** *80*, 1339.
31. Zhan, Y. H.; Xia, H. S.; Yuan, G. P. *Macromol. Mater. Eng.* **2011, 296.**
32. Hong, J. S.; Namkung, H. K.; Ahn, H. S.; Lee, J.; Kim, C. *Polymer* **2006,** *47*, 3967.
33. Kelnar, I.; Khunova, V.; Kotek, J.; Kapralkova, L. *Polymer* **2007,** *48*, 5332.
34. Zou, H.; Wang, K.; Zhang, Q.; Fu, Q. *Polymer* **2006,** *47*, 7821.
35. Potschke, P.; Kretzschmar, B.; Janke, A. *Compos. Sci. Technol.* **2007,** *67*, 855.
36. Ahmad, I.; Ismail, R.; Abdullah, I. *Polym. Eng. Sci.* **2011,** *51*, 419.
37. Sahebian, S.; Zebarjad, S. M.; Sajjadi, S. A. *J. Mater. Process. Tech.* **2009,** *209*, 1310.
38. Wunderlich, B. Macromolecular Physics; Academic Press: New York, **1980.**
39. Baltá-Calleja, F. J.; Vonk C. G. X-ray Scattering of Synthetic Polymers; Elsevier publishers: Amsterdam, **1989.**